RSC Advances

ROYAL SOCIETY OF CHEMISTRY

www.rsc.org/advances

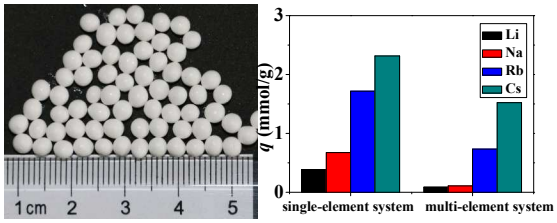

The adsorption of alkali metal ions onto the synthesized $Ca(ALG)_2$-$KB(C_6H_5)_4$ beads follows a sequence of $Cs^+ > Rb^+ >> Na^+ \sim Li^+$.

Competitive adsorption of Li, Na, K, Rb, Cs ions onto calcium alginate-potassium tetraphenylborate composite adsorbent

Tan Guo[ab], Yaoqiang Hu[ab], Xiaolei Gao[ab], Xiushen Ye[a], Haining Liu*[a] and Zhijian Wu*[a]

[a] *Laboratory of Salt Lake Resources Chemistry, Qinghai Institute of Salt Lakes, Chinese Academy of Sciences, Xining 810008, China*
[b] *University of Chinese Academy of Sciences, Beijing 100049, China*

Abstract: In this study, the calcium alginate-potassium tetraphenylborate ($Ca(ALG)_2$-$KB(C_6H_5)_4$) composite adsorbent was synthesized using potassium tetraphenylborate ($KB(C_6H_5)_4$) as the adsorption-active component and calcium alginate ($Ca(ALG)_2$) as the matrix material. Different techniques were used for characterization of the adsorbent such as SEM, EDS, XRD, laser particle size analyzer and moisture analyzer. Competitive adsorption of Li, Na, K, Rb, Cs ions onto the adsorbent was investigated through kinetic curves, adsorption isotherm and column techniques at 25°C. The equilibrium adsorption capacities were compared in the single-element and multi-element systems. The equilibrium adsorption amount was in the sequence of Cs^+ > Rb^+ >> Na^+ ~ Li^+, and Li and Na ions were hardly adsorbed. The separation factor was found to follow the order of $\beta_{Cs/Li}>\beta_{Rb/Li}>\beta_{Na/Li}$ under both the noncompetitive and competitive adsorption conditions. In the kinetic experiments for competitive adsorption, the adsorption reached equilibrium in about 24 h. The equilibrium sorption data were described by the Langmuir and Freundlich isotherm models and the results showed that the Langmuir model with determination coefficients of 0.997 and 0.981 for Cs^+ and Rb^+ respectively could describe the competitive system at room temperature more correctly. The lower breakthrough ratio and higher adsorption amount were observed for Cs^+ in the column experiments for competitive adsorption. The ion-exchange was deduced as the mechanism for selective adsorption of Rb^+ and Cs^+ ions onto the composite on the basis of EDS and XRD analysis of the adsorbent before and after adsorption. The tetraphenylborate anion ($B(C_6H_5)_4^-$) had different affinity to different alkali metal ions following the order of Cs^+ > Rb^+ > K^+ due to the order of solubility product *Ksp* ($CsBph_4$) < *Ksp* ($RbBph_4$) < *Ksp* ($KBph_4$).

Key words: Alkali metal ion; Rubidium; Cesium; Calcium alginate-potassium tetraphenylborate; Competitive adsorption

Introduction

Rubidium and cesium as highly dispersed and precious metal elements are extraordinarily significant resources. They have played an important role in many fields. In health care, rubidium and cesium can be used to treat nerve atrophy, tumor and cancer.[1,2] They are also used for manufacturing photocell, spectrograph and scintillation detector because of their excellent optical and electronical properties.[3-5] The metals or compounds of rubidium and cesium which have a good catalytic effect

on hydrogenation and cracking reactions are widely used in biological and chemical areas.[6] In addition, they are extensively studied as a thruster in aviation sciences, as a atomic clock in navigation systems,[7] as a magnetic fluid in power generation technologies, etc..

Radioactive cesium is also of great concern in the environment, public health, and safety aspects. ^{137}Cs with a half life of 30.5 years is a fission product typically present in the nuclear spent fuel. The well-known examples are radiological accidents in 1986 in Chernobyl[8,9] and in 2011 in Fukushima[10,11] where many people were injured and the environment became contaminated. So it is crucial to dispose ^{137}Cs by means of separation materials possessing strong adsorption ability.

Under natural conditions, rubidium and cesium exist in the salt lake, geothermal water and oil field brine besides ore minerals. Rubidium and cesium as the accompanying elements usually coexist with other alkali metals such as lithium, sodium and potassium in the widespreadly distributed liquid resourses. Separation and extraction of these coexisting elements have been one of the most difficult problems due to their close similarity in physical and chemical characteristics. Adsorption is one of the effective methods to separate or extract rubidium and cesium from aqueous solutions. Current studies on the adsorption of alkali metal ions are mainly focused on the adsorption of one kind of alkali metal ion, especially lithium or cesium ion.[12,13] However, the adsorption of rubidium and cesium ions would be affected by the presence of other alkali metal ions. Therefore, it is necessary to investigate the competitive adsorption behavior of the alkali metal ions in multi-element aqueous solutions.

In order to find a specific material for the effective separation of alkali metal ions, we describe a simple method to produce $Ca(ALG)_2$-$KB(C_6H_5)_4$ composite adsorbent by the sol-gel process. In this paper, the adsorbent was characterized by different methods such as SEM, EDS, XRD, laser particle size analyzer and moisture analyzer. Investigation was performed on the adsorption behavior of the typical coexistent ions Li^+, Na^+, K^+, Rb^+ and Cs^+ onto the adsorbent.

Experimental

Materials

Lithium chloride, sodium chloride, potassium chloride, rubidium chloride, cesium chloride and calcium chloride purchased from Tianjin Baishi Chemical Industry Co. Ltd., China. Sodium tetraphenylborate and sodium alginate were supplied from Shanghai Chemical Reagent Co. Ltd. and Sinopharm Chemical Reagent Co. Ltd., respectively. All reagents were analytical grade except for sodium alginate (Chemical Grade) without further purification. All aqueous solutions were prepared with water that had been purified.

Preparation of the Composite Adsorbent

The powder of potassium tetraphenylborate ($KB(C_6H_5)_4$) as the adsorption-active

component was freshly prepared by the following procedures. Firstly, the $KB(C_6H_5)_4$ suspension was prepared through precipitation by mixing 30 mL 1.0 mol/L KCl solution and 100 mL 10% $NaB(C_6H_5)_4$ solution under stirring. Then this suspension was dried for 48 h at 40°C to remove water and ground into powder.

During the preparation of calcium alginate-potassium tetraphenylborate ($Ca(ALG)_2$-$KB(C_6H_5)_4$) composite adsorbent, 10 g $KB(C_6H_5)_4$ powder was dispersed into 100 mL 2% sodium alginate (NaALG) solution under stirring to get uniform suspensions. These suspensions were pumped dropwise into 200 mL 4% $CaCl_2$ solution by a syringe to obtain composite gel beads. The gel beads were filtered from the solutions after aging 48 h. Successively, they were washed several times with distilled water till no Cl^- and then stored in distilled water. The wet composite gel beads defined as $Ca(ALG)_2$-$KB(C_6H_5)_4$ were used for the adsorption experiments. Before use, the beads were collected and the water in excess of the adsorbent surface was adsorbed by filter papers.

Characterization of the Composite Adsorbent

The SEM image of the powder of $KB(C_6H_5)_4$ was taken on a JSM-5610LV SEM instrument (JEOL Ltd., Japan). Before taking the SEM image the adsorbents were coated with a thin gold film. The powder particle size of the prepared $KB(C_6H_5)_4$ was determined by laser particle size analyzer (BT-9300S, Dandong Baite Instruments Co., Ltd., China). The water content of the wet composite adsorbent was determined by a MB45 moisture analyzer (Ohaus Corporation, Switzerland). The composite adsorbent before and after adsorption was dried at 40°C and grinded into powder, used to obtain the EDS spectra and XRD patterns. The EDS spectra of the adsorbents were obtained with an Oxford INCA instrument (Oxford Instrument Co., Ltd., UK). The XRD patterns were collected on an X'Pert PRO (PANalytical) diffractometer using Cu K_α radiation (λ = 0.15419 nm) over a 2θ range from 5° to 80°.

Adsorption Experiments

The batch adsorption experiments were performed by mixing 2 g wet $Ca(ALG)_2$-$KB(C_6H_5)_4$ adsorbent with 50 mL alkali metal ions solutions at 25 °C in a water bath (SHA-C; Changzhou Guohua Co., Ltd., China) with a shaking speed of 155 rpm. In the single-element systems for the noncompetitive adsorption experiments, the metal ion concentration was 0.01 mol/L. In the multi-element systems for the competitive adsorption experiments, each of Li, Na, K, Rb, and Cs metal ion concentration was 0.01 mol/L (i.e., total metal concentration was 0.05 mol/L). While in adsorption isotherms experiments, each of alkali metal ion concentration was 0.002 mol/L, 0.004 mol/L, 0.008 mol/L, 0.01 mol/L, 0.02 mol/L, 0.04 mol/L, respectively. The dynamic adsorption behaviors were studied in the ion exchange column, which was packed with 10 g wet $Ca(ALG)_2$-$KB(C_6H_5)_4$ beads passing by the multi-element solution from top to bottom. The flow rate of feed solution was adjusted by a peristaltic pump at 0.16 mL/min. During loading run, the column effluent samples were collected periodically and analyzed. The loading run was continued till saturation breakthrough was reached.

The concentration of alkali metal ions was determined using an ICS-1100 ionic chromatograph (Dionex Corporation).The adsorption amount of the alkali metal ions onto the composite adsorbent was calculated by the equation (1).

$$q = \frac{V(C_0 - C)}{m} \quad (1)$$

where q is the adsorption amount of metal ions onto the $Ca(ALG)_2$-$KB(C_6H_5)_4$ beads (mmol/g) at time t, V is the volume of the solution (L), m is the mass of the dry weight of the adsorbent (g), C_0 and C are metal ions concentration in solutions at beginning and time t (mmol/L), respectively. When the equilibrium solution concentration C_e was instead of C, the equilibrium adsorption amount q_e was obtained.

Results and Discussion

Characterization of the Adsorbents

The SEM image was focused on $KB(C_6H_5)_4$ powder, which the particles' size and surface morphology were uniform as shown in Fig. 1. The median diameter of prepared $KB(C_6H_5)_4$ powder was 1.7-2.5 μm determined by laser particle size analyzer as shown in Fig. 2.

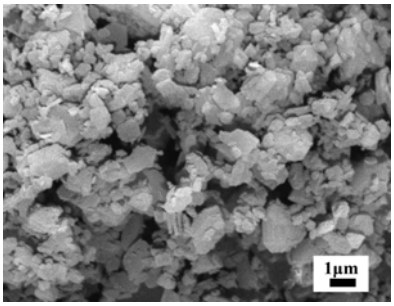

Fig. 1 SEM images of potassium tetraphenylborate powder.

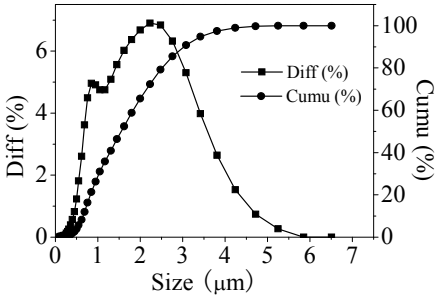

Fig. 2 The size distribution of potassium tetraphenylborate powder.

Fig. 3 The photograph of the composite adsorbent.

The diameter of the wet $Ca(ALG)_2$-$KB(C_6H_5)_4$ beads ranged from 2 mm to 4 mm as shown in Fig. 3. $KB(C_6H_5)_4$ was insufficient for handing column operation and solid-liquid separation because of its fine powder form. So the powder was granulated by alginate gel polymers for the practical separation process. The water content of the wet composite adsorbent was determined to be 85.66%, which was less than that of pure $Ca(ALG)_2$ gel beads prepared in the same way (96.22%), due to the effective entrapment of potassium tetraphenylborate.

Comparison of the Adsorption Capacities in Noncompetitive and Competitive Systems

The results for the noncompetitive and competitive adsorption of $Ca(ALG)_2$-$KB(C_6H_5)_4$ were shown in Fig. 4. As shown in Fig. 4, the equilibrium adsorption amount was found to follow the order of $Cs^+ > Rb^+ >> Na^+ \sim Li^+$ under both the noncompetitive and competitive adsorption conditions. And noncompetitive adsorption amount of different alkali metal ions is higher than the competitive adsorption owing to stronger ion strength in competitive system.[14,15]

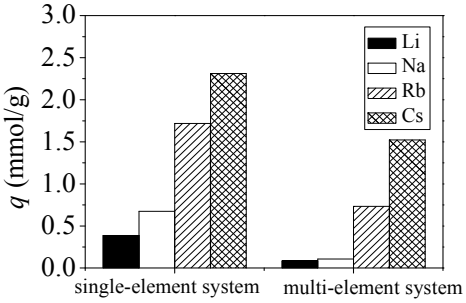

Fig. 4 Equilibrium adsorption amount comparison of $Ca(ALG)_2$-$KB(C_6H_5)_4$ for the noncompetitive and competitive adsorption.

In order to have a total comparison for the adsorption, separation factors were calculated according to the equation (2) based on adsorption equilibrium data,

$$\beta_{M/Li} = \frac{q_M / C_M}{q_{Li} / C_{Li}} \quad (2)$$

where *M* denotes Na, Rb, or Cs. The results are listed in Table 1.

Table 1 Separation factors for the adsorption under different conditions

conditions	$\beta_{Na/Li}$	$\beta_{Rb/Li}$	$\beta_{Cs/Li}$
single-element system	1.22	4.64	5.41
multi-element system	1.82	9.83	21.1

As shown in Table 1, competitive adsorption of different alkali metal ions present larger separation factor compared to the noncompetitive adsorption. The separation factor was found to follow the order of $\beta_{Cs/Li}>\beta_{Rb/Li}>\beta_{Na/Li}$ under both conditions. The order of preference for the adsorption is $Cs^+ > Rb^+ >> Na^+ \sim Li^+$. It was demonstrated that the composite adsorbent exhibited favorable selectivity for Cs^+ and Rb^+ especially in multi-element systems compared to the single-element systems.[16,17]

Adsorption Kinetic Curves under Competitive Conditions

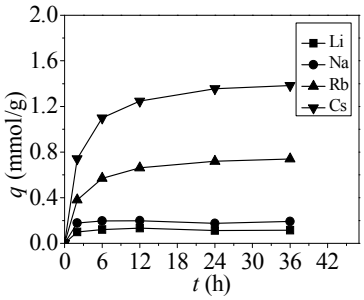

Fig. 5 Kinetic curves for competitive adsorption.

As shown in Fig. 5, the competitive adsorption was also found to reach equilibrium in about 24 h. At the beginning (t < 6 h), the adsorption amount increased rapidly, followed by a slow increase until the equilibrium was reached. The rapid increase was probably owing to the abundant availability of active sites on the adsorbent.[18] As time passed, theses sites were gradually occupied by Rb^+ or Cs^+, so the sorption became slower and quantitatively insignificant.

Adsorption Isotherms Results under Competitive Conditions

The isotherms for the competitive adsorption at 25°C were shown in Fig. 6.

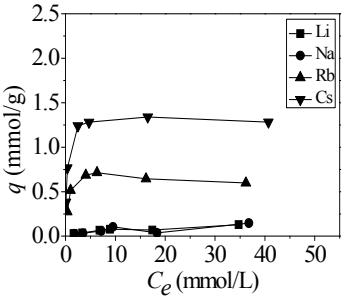

Fig. 6 Adsorption isotherms for the competitive adsorption.

The correlation of the concentration between alkali metal ions adsorbed on the

adsorbent and remained in solution is described by isotherms models. The experimental data about Cs^+, Rb^+ were fitted with Langmuir isotherm model based on monolayer adsorption[19,20] and Freundlich isotherm model based on multilayer adsorption.[21,22]

The Langmuir isotherm model is expressed as the equation (3),

$$\frac{1}{q_e} = \frac{1}{q_m} + \left(\frac{1}{bq_m}\right)\left(\frac{1}{C_e}\right) \quad (3)$$

where q_e is the equilibrium adsorption amount (mmol/g), C_e is the amount of Cs^+ or Rb^+ remaining in solution at equilibrium (mmol/L), q_m is the maximum adsorption capacity (mmol/g) and b is Langmuir constant (L/mmol). q_m and b can be determined from the slope and the intercept of $1/q_e$ vs. $1/C_e$ line plot as shown in Fig. 6.

The Freundlich isotherm model is given by the equation (4),

$$\log q_e = \log k + \frac{1}{n}\log C_e \quad (4)$$

where q_e is the equilibrium adsorption amount (mmol/g), C_e is the amount of Cs^+ or Rb^+ remaining in solution at equilibrium (mmol/L), k and n both are Freundlich constants which can be determined from the slope and the intercept of $\log q_e$ vs. $\log C_e$ line plot as shown in Fig. 7.

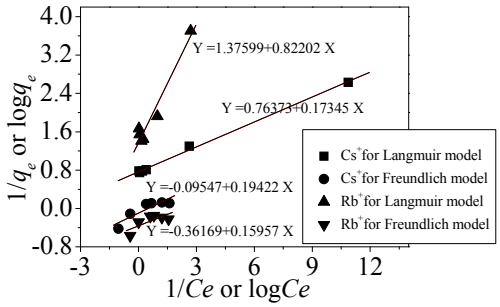

Fig. 7 Adsorption isotherm models with experimental results for Isotherms for Cs^+, Rb^+ adsorption.

As shown in table 2, the R^2 values of Langmuir isotherm model were very close to unity, but the R^2 values of Freundlich isotherm model deviated from unity seriously, proving the nice fitting of Langmuir isotherm model to these adsorption experimental data. The maximum sorption capacities q_m corresponding to complete monolayer coverage were 1.32 mmol/g and 0.73 mmol/g for Cs^+, Rb^+ on $Ca(ALG)_2$-$KB(C_6H_5)_4$ beads, respectively.

Table 2 The values of model parameters and R^2 for Cs^+, Rb^+ adsorption

ion	Langmuir model			Freundlich model		
	q_m (mmol/g)	b (L/mmol)	R^2	k (mmol/g)	n	R^2
Cs^+	1.32	4.46	0.997	0.80	5.26	0.791
Rb^+	0.73	1.67	0.981	0.43	6.25	0.559

Dynamic Adsorption Behaviors under Competitive Conditions

Fig. 8 represents the results of column experiments in the form of breakthrough curves for Li, Na, Rb and Cs ions. The breakthrough ratio of ions is C/C_0, where C is

alkali metal ion concentration of the effluent solution and C_0 is concentration of the feed solution.

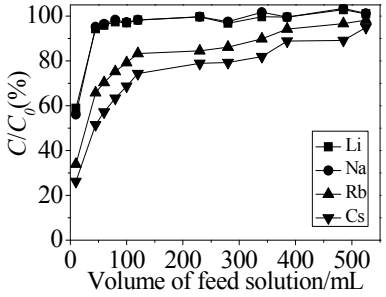

Fig. 8 Breakthrough curves for the competitive adsorption. The inner diameter was 1.2 cm and the height was 24 cm of the column.

In the case of 0.01 mol/L Li^+, Na^+, K^+, Rb^+, Cs^+ (total metal concentration was 0.05 mol/L) bearing feed, the breakthrough of alkali metal ions occurred at 10 mL volume. Thereafter, increasing amounts of ions were found in the effluent and the column reached saturation after passing 45 mL feed solution for Li^+, Na^+ and 530 mL for Rb^+, Cs^+. Li and Na ions were hardly adsorbed in the column experiments. The order of C/C_0 was $Li^+ \sim Na^+ < Rb^+ < Cs^+$, so the lower breakthrough ratio was obtained for Cs^+ adsorption.

Fig. 9 represents the relation between the adsorption amount and breakthrough ratio of Rb^+, Cs^+ for column experiments. The adsorption amount of column experiments was calculated by the equation (5). The adsorption amount curves were obtained by means of integral from breakthrough data.

$$\int dq = \int \frac{(C_0 - C)}{m} dV \tag{5}$$

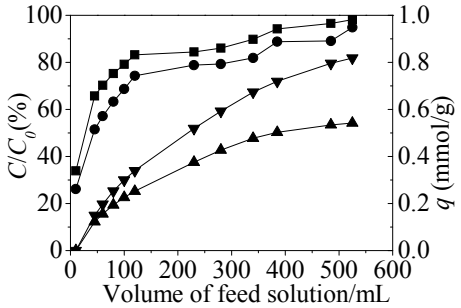

Fig. 9 Adsorption amount and breakthrough curves for Rb^+, Cs^+ in the competitive system. The inner diameter was 1.2 cm and the height was 24 cm of the column. (■Breakthrough of Rb^+ ●Breakthrough of Cs^+ ▼Adsorption amount of Cs^+ ▲Adsorption amount of Rb^+)

When the feed solution passed 530 mL, the breakthrough ratios were 98% for Rb^+ and 94% for Cs^+, the adsorption amounts were 0.54 mmol/g for Rb^+ and 0.82 mmol/g for Cs^+, respectively. So the higher adsorption amount was obtained for Cs^+ adsorption.

Adsorption Mechanisms

Fig. 10 showed the Energy Dispersive Spectroscopy (EDS) of the dried composite adsorbent before and after adsorption. The main metal elements were potassium and

calcium before adsorption, while the composition changed to potassium, calcium rubidium and cesium after adsorption, indicating the successful adsorption. After adsorption, the peaks of strong Rb^+ and stronger Cs^+ appeared, while a small amount of K^+ still existed, demonstrating that tetraphenylborate anion ($B(C_6H_5)_4^-$) had higher affinity to Cs^+ and $KB(C_6H_5)_4$ was uncompletely converted into $CsB(C_6H_5)_4$ and $RbB(C_6H_5)_4$.[23]

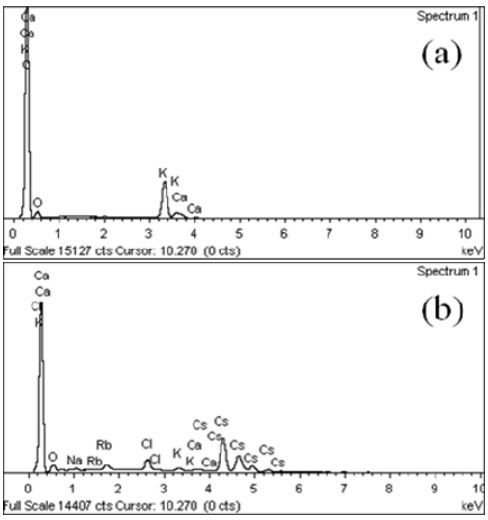

Fig. 10 The EDS patterns of the adsorbent before (a) and after (b) adsorption. For the adsorbent $Ca(ALG)_2$-$KB(C_6H_5)_4$, the EDS pattern after adsorption was obtained after adsorption for 24 h in the multi-element solution with concentration 0.02 mol/L of every alkali metal ion.

The XRD patterns of $KB(C_6H_5)_4$, $RbB(C_6H_5)_4$, $CsB(C_6H_5)_4$ from the references[24-26] and the adsorbent before and after adsorption were compared as shown in Fig.11. Fig. 11(b) showed that diffraction peaks of the adsorbent had changed between 10° and 20° besides 20° and 30° before and after adsorption. According to Fig. 11(a), the adsorbent before adsorption was the $KB(C_6H_5)_4$, and became to almost $CsB(C_6H_5)_4$ after adsorption.

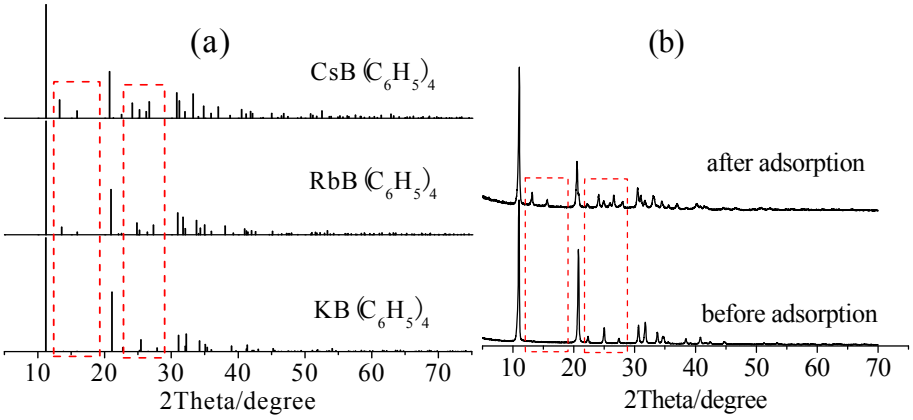

Fig. 11 The XRD patterns of standards (a) of $KB(C_6H_5)_4$, $RbB(C_6H_5)_4$, $CsB(C_6H_5)_4$ and the adsorbent before and after adsorption(b).

It was caused by the ion exchange reaction between Cs^+, Rb^+ and K^+ in the adsorption processes.[27,28] The corresponding reaction could be expressed as the equation (6), (7).

$$Ca(ALG)_2\text{-}K^+B(C_6H_5)_4^- + Cs^+ = Ca(ALG)_2\text{-}Cs^+B(C_6H_5)_4^- + K^+ \quad (6)$$

$$Ca(ALG)_2\text{-}K^+B(C_6H_5)_4^- + Rb^+ = Ca(ALG)_2\text{-}Rb^+B(C_6H_5)_4^- + K^+ \quad (7)$$

For the above content, The order of preference of alkali metal ions for $B(C_6H_5)_4^-$ is $Cs^+ > Rb^+ > K^+$, which is interpreted by the order of solubility product constants for tetraphenylborate salts, *Ksp* ($CsB(C_6H_5)_4$) (1.58×10^{-9}) < *Ksp* ($RbB(C_6H_5)_4$) (2.89×10^{-9}) < *Ksp* ($KB(C_6H_5)_4$) (3.06×10^{-8}) in detail.[29,30]

Conclusions

The composite adsorbent, $Ca(ALG)_2\text{-}KB(C_6H_5)_4$ was prepared and characterized. Competitive and noncompetitive adsorption of Li, Na, K, Rb, Cs ions onto the $Ca(ALG)_2\text{-}KB(C_6H_5)_4$ beads was investigated in batch experiments. The main results of our study could be summarized as follows:

(1) The prepared composite adsorbent was white beads. The size and surface morphology were uniform of the $KB(C_6H_5)_4$ powder and $Ca(ALG)_2\text{-}KB(C_6H_5)_4$ beads.

(2) Compared to the noncompetitive adsorption, competitive adsorption of different alkali metal ions presented differences in adsorption capacities. The equilibrium adsorption amount was found to follow the order of $Cs^+ > Rb^+ >> Na^+ \sim Li^+$, and Li and Na ions hardly were adsorbed. The separation factor was found to follow the order of $\beta_{Cs/Li}>\beta_{Rb/Li}>\beta_{Na/Li}$ under both the noncompetitive and competitive adsorption conditions.

(3) In the kinetic experiments for competitive adsorption, the adsorption reached equilibrium in about 24 h.

(4) The adsorption was fitted Langmuir isotherm model preferably for Cs^+ and Rb^+ in the competitive system.

(5) In the column experiments, the lower breakthrough ratio and higher adsorption amount were obtained for Cs^+.

(6) Ion exchange reaction was the mechanism for Rb^+ and Cs^+ onto $Ca(ALG)_2\text{-}KB(C_6H_5)_4$ beads. Compared to Rb^+ and K^+, $B(C_6H_5)_4^-$ had higher affinity to Cs^+ due to differences of the solubility product, that is *Ksp* ($CsBph_4$) < *Ksp* ($RbBph_4$) < *Ksp* ($KBph_4$).

Acknowledgements

This work was financially supported by the Foundation of Knowledge Innovation Program of Chinese Academy of Sciences (KZCX2-EW-QN309), the Western Action Program, Chinese Academy of Sciences (KZCX2-XB3-06), National Natural Science Foundation of China (51002164), the Foundation of Basic Research for Application of Qinghai Province (2013-Z-706) and “Western Light” Talents Training Program of Chinese Academy of Sciences (2011(2)).

References

1 H.E. Sartori, *Pharmacol. Biochem. Be.*, 1984, **21**, 11.

2 J. Zhong, W. Yao and W. Lee, *Int. J. Dev. Neurosci.*, 2007, **25**, 359.

3 V.S. Khazanov and S.G. Iurov, *Soviet physics: technical physics*, 1956, **1**, 1141.
4 E.I. Burmakin, G. Sh. Shekhtmang and E.I. Volegova, RU2415496 C1, 2011.
5 K.K. Toshiba, JP2001284662-A, 2002.
6 Y. Kano, M. Ohshima, H. Kurokawa and H. Miura, *React. Kinet., Mech. Catal.*, 2013, **109**, 29.
7 Th. Udem, R. Holzwarth and Th. Hänsch, *Eur. Phys. J.*, 2009, **172**, 69.
8 E.M. Korobova and S.L. Romanov, *Chemom. Intell. Lab. Syst.*, 2009, **99**, 1.
9 M.I. Balonov, L.R. Anspaugh, A. Bouville and I.A. Likhtarev, *Radiat. Prot. Dosim.*, 2007, **127**, 491.
10 P. Thakur, S. Ballard and R. Nelson, *Sci. Total Environ.*, 2013, **458-460**, 577.
11 J.A. Caffrey, K.A. Higley, A.T. Farsoni, S. Smith and S. Menn, *J. Environ. Radioactiv.*, 2012, **111**, 120.
12 X.F. Fan, W.T. Zheng, J.L. Kuo and D.J. Singh, *ACS Appl. Mater. Inter.*, 2013, **5**, 7793.
13 C.K. Kim, J.Y. Kong, B.S. Chun and J.W. Park, *Environ. Earth Sci.*, 2013, **68**, 2393.
14 S.C. Tsai, T.H. Wang, M.H. Li, Y.Y. Wei and S.P. Teng, *J. Hazard. Mater.*, 2009, **161**, 854.
15 C.X. Liu, J.M. Zachara, S.C. Smith, J.P. Mckinley and C.C. Ainsworth, *Geochimi. Cosmochim. Ac.*, 2003, **67**, 2893.
16 L.J. Li, F.Q. Liu, X.S. Jing, P.P. Ling and A.M. Li, *Water Res.*, 2011, **45**, 1177.
17 P. Srivastava, B. Singh and M. Angove, *J. Colloid Interf. Sci.*, 2005, **290**, 28.
18 R.R. Sheha and E. Metwally, *J. Hazard. Mater.*, 2007, **143**, 354.
19 M.M. Abd El-Latif and M.F. Elkady, *Desalination*, 2010, **255**, 21.
20 M.Y. Miah, K. Volchek, W. Kuang and F.H. Tezel, *J. Hazard. Mater.*, 2010, **183**, 712.
21 C. Dwivedi, A. Kumar, K.K. Singh, A.K. Juby, M. Kumar, P.K. Wattal and P.N. Bajaj, *J. Appl. Polymer Sci.*, 2013, **129**, 152-160.
22 D.H. Ding, Y.X. Zhao, S.J. Yang, W.S. Shi, Z.Y. Zhang, Z.F. Lei and Y.N. Yang, *Water Res.*, 2013, **47**, 2563.
23 R.Q. Li, R.E.K. Winter, J. Kramer and G.W. *Gokel, Supramol. Chem.*, 2010, **22**, 73.
24 A.L. Rheingold, J.A. Golen, Calculated from CSD using POWD-12++, *Private Communication*, 2005.
25 B. Wilde, F. Olbrich, Calculated from CSD using POWD-12++, *Private Communication*, 2005.
26 J.C. Bryan, Calculated from CSD using POWD-12++, *Z. Kristallogr.-New Cryst. Struct.*, 2000, **215**, 621.
27 C.Y. Chang, L.K. Chau, W.P. Hu, C.Y. Wang and J.H. Liao, *Micropor. Mesopor. Mat.*, 2008, **109**, 505.
28 C.L. Neskovic, S. Ayrault, V. Badillo, B. Jimenez, E. Garnier, M. Fedoroff, D.J. Jones and B. Merinov, *J. Solid State Chem.*, 2004, **177**, 1817.
29 A. Berne, B. Wajsbrot, P.D. Klahr and O. Popovych, *J. Chem. Eng. Data*, 1983, **28**, 316.
30 X.L. Wang, L.Z. Zou, P.J. Zhang, F.G. Wang, Q.J. Yu and B.X. Zhou, *J. Chem. Thermodyn.*, 1999, **31**, 1609.